# Mesenchymal stem cells (MSCs) generated using mRNA reprogramming show enhanced growth potential, secretome, and therapeutic efficacy in a demyelinating disease model

Jasmine K Harris[1], Christopher Rohde[2], Matthew Angel[2]
[1]Novellus, Inc., [2]Factor Bioscience Inc.

## Abstract

MSCs have undergone extensive clinical testing for many diseases and have consistently demonstrated safety. While the immuno-modulatory properties of MSCs have been well characterized, adult-tissue -derived MSCs have shown limited therapeutic efficacy, significant variability among samples, and limited proliferative capacity.
Here we explore induced pluripotent stem cells (iPSCs) as an alternative source of MSCs to potentially overcome these limitations.

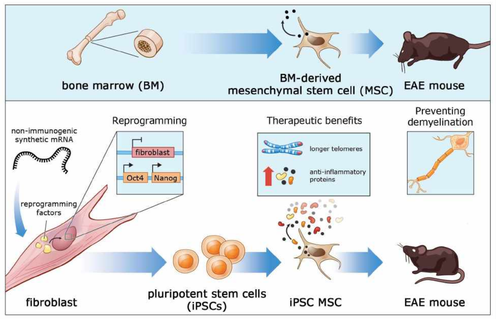


## Introduction

MSCs have shown effectiveness in treating inflammatory diseases such as multiple sclerosis (MS) and acute respiratory distress syndrome (ARDS). ARDS is of growing concern in the light of the COVID-19 coronavirus pandemic. ARDS is characterized by extensive inflammation in the lungs, causing severe shortness of breath. MSCs sourced from bone marrow, umbilical cord tissue, and adipose tissue are all being considered as possible therapies to treat ARDS. However, the ability to scale-up MSC manufacturing to meet the needs of the current crisis remains an open challenge. MSCs derived from iPSCs (iMSCs) offer a near limitless supply of cell due to their superior expansion potential.

## mRNA Reprogramming

iPSCs were generated from adult human fibroblasts derived from a dermal punch biopsy through a one-week, high-efficiency, immunosuppressant-free reprogramming protocol using mRNA encoding Oct4, Sox2, Klf4, c-Myc, and Lin28.


**Fig. 2 *Reprogramming Efficiency.* >6% efficiency was achieved using mRNA reprogramming. 1000 cells/well were plated on day 0; colonies were stained for SSEA4 on day 20.**

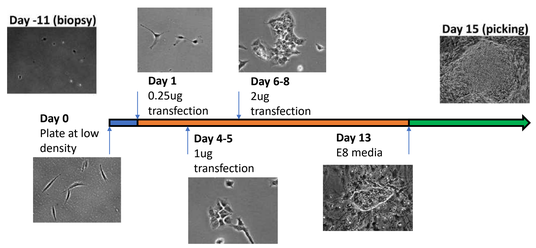


**Fig. 1 *Reprogramming Timeline.* Cells are shown from point of biopsy at day -11 to colony picking at day 15. 1000 cells were plated on day 0. On days 1 and 4-8 a transfection of synthetic mRNA was done. Colonies were picked after day 15.**

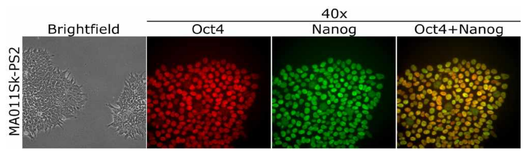


**Fig. 3 *Expression of Pluripotency Factors.* mRNA-reprogrammed cells (MA011sk PS2) were picked and cultured before being fixed with 4% Paraformaldehyde, permeabilized with triton, and then blocked with casein. Cells were stained for Oct4 and Nanog.**

## iMSC Characterization

iMSCs were generated using a 28 day high-yield monolayer protocol (Fig. 4).

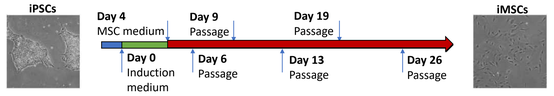


**Fig. 4 *MSC Differentiation Timeline*. iMSCs were generated using the STEMdiff Mesenchymal Progenitor Kit (STEMCELL Technologies). iPSCs were plated at a high density on day -2. Cells were cultured in induction media from day 0-4. On day 4 the media was changed to MesenCult ACF-Plus media.**

The iMSCs were characterized for gene expression by rtPCR (Fig. 6) and antibody staining (Fig. 5). Both showed loss of pluripotency factor expression. The rtPCR results also showed differences in the gene expression between iMSCs and BM-MSCs (Fig. 6).

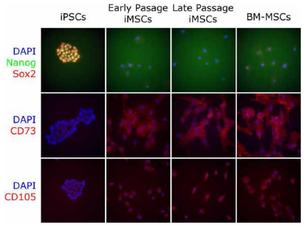


**Fig. 5 (above) *iMSC Surface-Marker Expression.* iPSCs, early and late passage iMSCs, and BM-MSCs were cultured, fixed with 4% paraformaldehyde, permeabilized with triton, blocked with casein, and stained for Nanog, Sox2, CD73, and CD105 (Endoglin). iMSCs and BM-MSCs stained negative for Nanog and Sox2 and the positive for the MSC markers CD73 and CD105.**

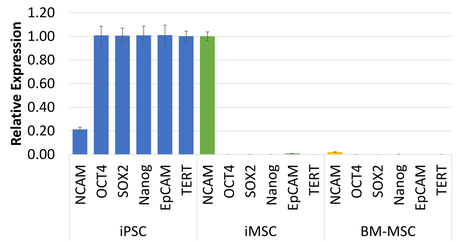


**Fig. 6 *iMSC Gene Expression.* RNA was extracted from iPSCs, iMSCs, and BM-MSCs, and was analyzed by rtPCR. Pluripotency factors (OCT4, SOX2, NANOG, and EpCAM) were downregulated in both iMSCs and BM-MSCs, while NCAM was upregulated in iMSCs, but downregulated in BM-MSCs.**

Multipotency of the iMSCs was assessed by differentiating into adipocytes, osteoblasts, and chondrocytes (Fig. 7).


**Fig. 7 *Differentiation of iMSCs.* iMSCs were differentiated using STEMCELL Technologies kits: MesenCult Osteogenic Differentiation Kit (Human), MesenCult-ACF Chondrogenic Differentiation Medium, MesenCult Adipogenic Differentiation Medium (Human).**

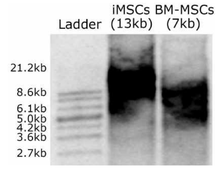


**Fig. 8 *iMSC Telomere Length.* The telomere lengths of iMSCs and BM-MSCs were measured using the TeloTAGGG Telomere Length Assay (Sigma). The telomere length of iMSCs was 13kb compared to 7kb for BM-MSCs.**

The telomere length of the BM-MSCs and the iMSCs were measured by Southern blot (Fig. 8). The telomere length of iMSCs were Found to be 6kb greater than that of BM-MSCs, suggesting that the telomeres were restored by the reprogramming process.

The proliferative capacity of iMSCs was determined by serial passaging until the onset of senescence (Fig. 9). iMSCs underwent >70 population doublings, while both research- and clinical-grade BM-MSCs reached senescence after fewer than 20 population doublings.

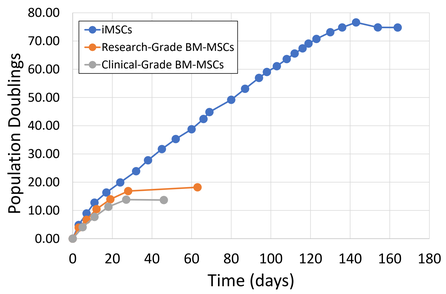


**Fig. 9 *iMSC Growth Curve.* iMSCs, BM-MSCs, and clinical-grade BM-MSCs were expanded in MesenCult-ACF Plus on Animal Component-Free Cell Attachment Substrate (STEMCELL Technologies). The cells were harvested using TrypLE Select CTS and Defined Trypsin Inhibitor (ThermoFisher). Cells were counted by Trypan Blue. The population doublings were determined using the extrapolated total number of cells. The iMSCs underwent 74.8 population doublings before senescence compared to 18.2 population doublings for the BM-MSCs.**

Comparative secretome analysis was performed using multiplex ELISA to determine levels of cytokines, chemokines, and growth factors known to be involved in inflammation. iMSCs showed overexpression of multiple potentially neuroprotective and anti-inflammatory factors, including CXCL1VEGF-A and CXCL5.

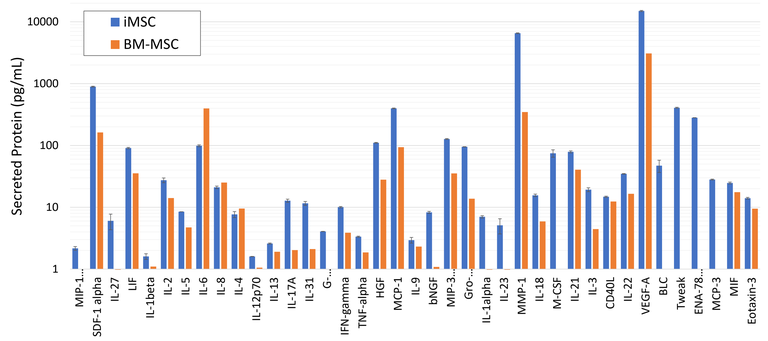


**Fig. 10 iMSC *Secretome Analysis.* Secreted protein levels were measured using the Immune Monitoring 65-Plex Human ProcartaPlex Panel (ThermoFisher). iMSCs showed 7-fold higher levels of CXCL1 and 4-fold higher levels of VEGF-A. CXCL5 was only detected in iMSCs.**

iMSC were further characterized using microarray gene-expression analysis (Fig. 11). Hierarchical clustering showed greater similarity between BM-MSCs and fibroblasts than iMSCs.

iMSCs were administered by tail-Vein injection to a MOG-induced EAE-mouse model (Fig. 12). Animals administered iMSCs showed delayed disease progression in comparison to animals administered BM-MSCs and a Disease-only control. These results suggest that iMSCs could be more effective in preventing the progression of diseases such as MS, and for other inflammatory diseases such as ARDS than MSCs derived from adult tissue.

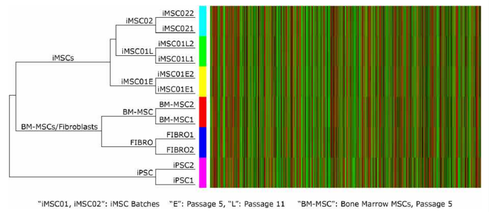


**Fig. 11 *Hierarchical Clustering Analysis* RNA was harvested from iPSCs, iPSC MSCs, and BM-MSCs then analyzed using the Whole Human Genome Oligo Microarray 4x44k from Agilent Technologies.**

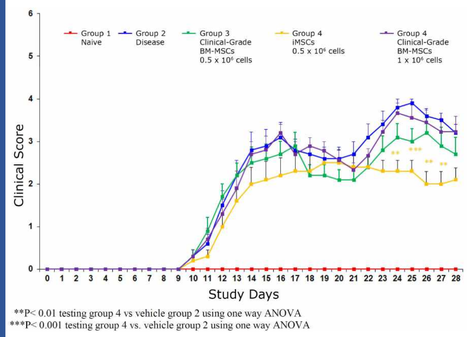


**Fig. 12 *iMSC in vivo Efficacy.* Experimental Autoimmune Encephelomyelitis (EAE) was induced in mice using MOG. The MOG injection was performed on study day 0 via an intravenous injection of 200ug MOG in 100uL PBS. Further immunostimulation was done by injecting 5 mL of pertussis toxin (PT) at 2ug/mL in PBS on study days 0 and 2. Cells were administered on study day 11 intravenously at a dose level of $0.5*10^6$ total cells in 200uL/mouse (and dose of $1*10^6$ for one of the clinical BM-MSC groups). Clinical score, which scores the severity of the disease progression on a scale from 0-5 with 5 being the most severe and 0 being unaffected. The iMSC group showed an improved clinical score compared to the disease-only control ($p < 0.001$).**

## Conclusions

Although BM-MSCs have shown excellent clinical safety, they have struggled to demonstrate therapeutic efficacy in many diseases of interest. High efficiency and lack of vector persistence make mRNA reprogramming an ideal platform for the development of new autologous and allogeneic MSC therapies. We show that iMSCs exhibit superior growth potential, secretome, and therapeutic efficacy in a demyelinating disease model when compared to BM-MSCs, suggesting that iMSCs may be an ideal cell therapy for devastating inflammatory diseases such as MS and ARDS.

JH, CR, and MA are inventors on U.S. Pat. Appl. No. 63,016,626. CR and MA are inventors on U.S. Pat. Nos. 8,497,124; 9,127,248; 9,399,761; 9,562,218; 9,695,401; 9,879,228; 9,969,983; 10,131,882; 10,201,599; 10,443,045; and others.